

On the statistical and transport properties of a non-dissipative Fermi-Ulam model

André L. P. Livorati, Carl P. Dettmann, Iberê L. Caldas, and Edson D. Leonel

Citation: *Chaos* **25**, 103107 (2015); doi: 10.1063/1.4930843

View online: <http://dx.doi.org/10.1063/1.4930843>

View Table of Contents: <http://scitation.aip.org/content/aip/journal/chaos/25/10?ver=pdfcov>

Published by the **AIP Publishing**

Articles you may be interested in

[On exact statistics and classification of ergodic systems of integer dimension](#)

Chaos **24**, 023125 (2014); 10.1063/1.4881890

[Dependence of advection-diffusion-reaction on flow coherent structures](#)

Phys. Fluids **25**, 106602 (2013); 10.1063/1.4823991

[Dynamics of some piecewise smooth Fermi-Ulam models](#)

Chaos **22**, 026124 (2012); 10.1063/1.3695379

[Dynamical properties of a dissipative hybrid Fermi-Ulam-bouncer model](#)

Chaos **17**, 013119 (2007); 10.1063/1.2712014

[Spectral properties and anomalous transport in a polygonal billiard](#)

Chaos **10**, 189 (2000); 10.1063/1.166493

Searching?
Trust
CiSE.

It's peer-reviewed and appears in the IEEE Xplore and AIP library packages.

python in scientific computing

Python for scientific computing
TE Oliphant - *Computing in Science & Engineering*, 2007 - scitation.org
By itself, Python is an excellent scripting language for scientific computing languages. However, with additional basic tools, Python transforms into a language suited for scientific and engineering code that's often faster than C. Cited by 690 Related articles All 12 versions Cite Save

IPython: a system for interactive scientific computing
F. Perez, BE Granger - *Computing in Science & Engineering*, 2007 - sciencedirect.com
... The Interactive Data Language (IDL) and Matlab (for numerical computing) comprehensive set of tools for building special-purpose interactive environments.

Scikit-learn: Machine learning in Python
E. Pedregosa, G. Varoquaux, A. Gramfort, ... - *The Journal of Machine Learning Research*, 2011 - jmlr.org
... Ki Mirmann and M. Avastis, editors: *Scientific Python*, volume 11 of *Computing in Science & Engineering*. ... The NumPy array: A structure for efficient numerical computation, *Computing in Science and Engineering*, 11, 2011. T. Zito, N. Wilbert, L. Wiskott, and P. Berkes, ...

On the statistical and transport properties of a non-dissipative Fermi-Ulam model

André L. P. Livorati,^{1,2,3} Carl P. Dettmann,³ Iberê L. Caldas,² and Edson D. Leonel^{1,4}

¹*Departamento de Física, UNESP - Univ. Estadual Paulista, Ave. 24A, 1515, Bela Vista, 13506-900 Rio Claro, SP, Brazil*

²*Instituto de Física, IFUSP - Universidade de São Paulo, Rua do Matão, Tr.R 187, Cidade Universitária, 05314-970 São Paulo, SP, Brazil*

³*School of Mathematics, University of Bristol, Bristol BS8 1TW, United Kingdom*

⁴*Abdus Salam International Center for Theoretical Physics, Strada Costiera 11, 34151 Trieste, Italy*

(Received 10 April 2015; accepted 31 August 2015; published online 14 September 2015)

The transport and diffusion properties for the velocity of a Fermi-Ulam model were characterized using the decay rate of the survival probability. The system consists of an ensemble of non-interacting particles confined to move along and experience elastic collisions with two infinitely heavy walls. One is fixed, working as a returning mechanism of the colliding particles, while the other one moves periodically in time. The diffusion equation is solved, and the diffusion coefficient is numerically estimated by means of the averaged square velocity. Our results show remarkably good agreement of the theory and simulation for the chaotic sea below the first elliptic island in the phase space. From the decay rates of the survival probability, we obtained transport properties that can be extended to other nonlinear mappings, as well to billiard problems. © 2015 AIP Publishing LLC. [<http://dx.doi.org/10.1063/1.4930843>]

We study the dynamics of an ensemble of non-interacting particles moving constrained by two infinitely heavy walls, where one of them is moving periodically in time and the other is fixed. This problem, also known as Fermi-Ulam model (FUM), has application in many areas, including astrophysics, atom-optics, quantum mechanics, among others. The diffusive behaviour of the velocity, here set as the way the transport of orbits occurs in the phase space, is investigated considering transport properties obtained from the decay rate of the survival probability, defined by means of escape formalism. Since the system present mixed dynamics, stickiness phenomenon may influence the transport causing anomalous diffusion. In this study, we developed an analytical approach for the diffusion coefficient along the transport through the chaotic sea considering escape rate formalism and survival probability analysis. The numerical results we obtained are in good agreement with the theory, and confirm the robustness of the formalism. The results obtained here can be extended to other similar dynamical systems.

the presence of cantori (fractal dimension tori),² and due to labyrinth islands and chains of islands, generated by resonances; orbits that are originated in the chaotic sea, may be trapped for around these stability structures for long finite time intervals. Such effect is caused by a dynamical trapping which is called stickiness.^{3,4} This finite trapping can cause irregular diffusion of particles where an intermittent behavior may occur, alternating between normal diffusion (chaotic behavior) and irregular (stickiness influence). The stickiness phenomenon was originally proposed in early 1970s, by Contopoulos⁵ in his study about galaxy dynamics. Nowadays, sticky orbits lead to a new scenario of modern science, where anomalous transport and statistical properties can be obtained in the dynamics of systems in different areas of research such as plasmas,^{6,7} acoustic,⁸ astronomy,⁹ biology,¹⁰ among others (see Ref. 11 for a review).

In this study, we propose to use diffusion and decay rates of the survival probability to investigate transport in the chaotic dynamical regime of the FUM.¹² The FUM was originally proposed by Ulam in early 60s,¹² as an attempt to produce a prototype that could explain the Fermi Acceleration¹³ (unbounded energy growth). The system consists of an ensemble of non-interacting particles confined to move between two infinitely heavy walls, which the particles collide elastically. One wall is assumed to be fixed while the other one oscillates periodically in time. Despite the simple mechanics of the model, it leads to a complex variety of nonlinear phenomena in both conservative and dissipative dynamics.^{14–18} Also, one may find applications of its dynamics in different areas of research as astrophysics,¹⁹ atom-optics,^{20,21} quantum effects,^{22–24} experimental devices,^{25,26} among others. The phase space of the system is mixed and contains both periodic islands surrounded by a chaotic sea which is limited by a set of invariant curves. The lower

I. INTRODUCTION

Typical dynamics of Hamiltonian systems are non-integrable and non-ergodic.¹ Such behavior leads the system to present mixed phase space, with chaotic seas, invariant tori, and Kolmogorov-Arnold-Moser (KAM) islands.² For strongly chaotic systems, the dynamics has a normal diffusive behavior, where particles move freely in the phase space like a Brownian motion.^{1,2} In a nearly integrable system, an initial condition started in the chaotic sea may present a very complicated behavior. Stability islands influence directly the dynamics generating anomalous effects in the transport properties for a chaotic orbit.³ In fact, owing to

one is analytically obtained as function of the control parameter²⁷ and works as a barrier blocking a flow of particles through it. This implies that we have a finite portion of the phase space for orbits to diffuse, and hence we have a mixed phase space dynamics; we are interested in studying how the diffusive process and transport occur for this region and if the survival probability analysis would give us transport coefficients related with the escape formalism already known in the literature.^{28–33}

In many scenarios, we are not interested in the individual behavior of an initial condition or particle, but rather in the average properties of the system, particularly when an ensemble of particles is taken into account.²⁸ This is the main reason to consider statistical techniques to evaluate the description of dynamical phenomena.^{29–33} An intuitive example is to drop some colored ink in water, and study how the particles of ink move far away from each other in the liquid surface when this is also moving. When a physical system is setup, a leakage can be considered as the introduction of a hole or even a barrier.^{34,35} We introduce a hole in the system, a pre-defined region, related to the dynamical variable in study, where orbits can escape through it.^{11,34,35} One can say, the probability density of an ensemble of initial conditions to survive this leaking is $\rho(\vec{r}, t)$, where \vec{r} represents a generic dynamical variable in study, for example, the action, where $\rho=0$ in the hole. Note that this is an approximate, coarse grained description, averaging over less relevant variables (the angle ϕ in our case). Consider we can separate the “dynamical region” in two parts: (i) particles that have escaped through the hole; and (ii) particles that still have not escaped. Hence, we can define a current of flow for the escape. Of course it must be proportional to the difference of concentration of particles among both regions. So, we may write $\vec{j}(\vec{r}, t) = -D\nabla\rho(\vec{r}, t)$, where D is the diffusion coefficient. Considering yet the continuity equation for conservation of particles, we have $\frac{\partial\rho(\vec{r}, t)}{\partial t} = -\nabla\cdot\vec{j}(\vec{r}, t)$, and combining both expressions, we obtain the diffusion equation

$$\frac{\partial\rho(\vec{r}, t)}{\partial t} = D\nabla^2\rho(\vec{r}, t). \quad (1)$$

A natural question is then raised about the decay rate of $\rho(\vec{r}, t)$. The main aspect of this analysis is that the escape rate is extremely sensitive to the dynamics of the system. For strongly chaotic systems, which present normal diffusion, the decay is typically exponential,^{11,28} while for systems that present mixed phase space, with irregular diffusion due stickiness influence, the decay can be slower, presenting a mix of exponential with a power law,^{11,36} or stretched exponential decay.^{37,38} Indeed, when a non-exponential decay is observed, the dynamics would require a long range correlation, as, for example, a consequence of stickiness influence.¹¹ An equally important aspect is that the escape rate can have a strong dependence on the position and size of the hole.^{39–41}

The investigation of the transport and of the diffusion properties of FUM is done by solving Eq. (1) considering boundary conditions for the escape in different hole positions along the phase space, particularly on the velocity axis.

Considering an ensemble of particles, when a particle reaches a hole, we consider it has escaped, and the time evolution of other particle from the ensemble is started. An analytical expression is obtained for the diffusion coefficient as function of the expansion in Fourier series.⁴² Our theoretical findings are compared with numerical simulations obtained via the average squared velocity. The agreement of the theory with the simulation for the lower region in the phase space is remarkably well confirming the robustness of the formalism. The formalism used could be extended to other systems described by discrete mappings, particularly the billiard dynamical systems.

The paper is organized as follows: In Sec. II, we describe the Fermi-Ulam model, its dynamical and some of its chaotic properties. Section III is devoted to discuss the analytical procedure and to solve the partial differential equation given in Eq. (1). We also do a comparison of the numerical results with the theory, confirming a good agreement of the two. Finally in Sec. IV, we present our final remarks and conclusions.

II. THE MODEL AND THE MAPPING

We start describing the model under consideration. It consists of a particle, or equivalently of an ensemble of non-interacting particles moving constrained by two infinitely heavy walls with an absence of gravitational field. Collisions are considered to be elastic, hence there is no fractional loss of energy upon collision. One wall is fixed at $x = \ell$ and works as a returning mechanism for the particle to suffer a further collision with a moving wall. This is described by a periodic oscillating function of the type $x_w(t) = \varepsilon \cos(\omega t)$, where ε and ω are, respectively, the amplitude and the frequency of oscillation. The dissipative dynamics is not from interest in this paper although it has been considered via inelastic collisions where a restitution coefficient was introduced to simulate the fraction loss of energy upon collision of the particles with the wall.¹⁶ Kinetic friction was also taken into account in the literature⁴³ as well as in-flight dissipation.⁴⁴

The dynamics of the system we are investigating is described by a two-dimensional, nonlinear, measure preserving discrete mapping for the variables velocity of the particle v and time t immediately after the n th collision of the particle with the moving wall. There are two distinct versions of the dynamics known in the literature: (i) the complete version; and (ii) static wall approximation. Case (i), i.e., the complete version, takes into account the full motion of the moving wall, leading the instant of each collision to be obtained via solution of transcendental equations. The static wall approximation, marked by case (ii), assumes both walls are fixed; however, after the impact with the one on the left, the particle experiences an exchange of energy and momentum as if the wall was moving. With such an approximation, the transcendental equations no longer need to be solved and, at the same time, the nonlinearity of the problem is kept. Such a version was very useful long time ago when computers were far slow. It also gives the huge advantage of making the analytical discussions easier as compared to the complete model. The scaling properties observed in the simplified

model²⁷ are also present in the complete version. In this paper and from this point and beyond, we consider only the complete version of the model. All of our analytical results were obtained using the complete model.

To construct the mapping, let us suppose the initial condition for a moving particle is v_0 and t_0 . We also assume that at $t = t_0$, the position of the particle is at $\epsilon \cos(\omega t_0)$. There are three control parameters, ϵ , ℓ , and w , and that not all of them are relevant for the dynamics. It is then convenient to define dimensionless and hence a more convenient set of variables. We define $V_n = v_n/w\ell$, $\epsilon = \epsilon/\ell$ and finally measure the time in terms of the number of oscillations of the moving wall $\phi_n = \omega t_n$. Starting with an initial condition (V_n, ϕ_n) with initial position of the particle given by $x_p(\phi_n) = \epsilon \cos(\phi_n)$, the dynamics is evolved by a map \tilde{T} which gives the pair (V_{n+1}, ϕ_{n+1}) in the $(n + 1)$ th collision with the moving wall. Taking these into account, we end up with the following mapping:

$$\tilde{T} : \begin{cases} V_{n+1} = V_n^* - 2\epsilon \sin(\phi_{n+1}) \\ \phi_{n+1} = [\phi_n + \Delta T_n] \bmod(2\pi). \end{cases} \quad (2)$$

The expressions for V_n^* and ΔT_n depend on what kind of collision happens: (i) multiple collisions and; (ii) single collisions. The multiple collisions are such that, after the particle enters in the collision zone, $x \in [-\epsilon, +\epsilon]$ and hits the moving wall, before it leaves the collision zone, the particle suffers a second and hence multiple collision. Further collisions can also be observed. They indeed are less probably to be observed. This implies that the probability of observing a second successive collision is smaller than observing one. Observing three successive is smaller than observing two and so on. In fact, such probability has the form $P(n_{sr}) \propto n_{sr}^{-3.76}$, where n_{sr} denotes the number of successive reflections. For a further discussion, see Ref. 45, which discusses such reflections in a periodically corrugated waveguide, a model which has topological similarities with the complete Fermi-Ulam model. The expressions for both V_n^* and ΔT_n are given by $V_n^* = -V_n$ and $\Delta T_n = \phi_c$. The numerical value of ϕ_c is obtained as the smallest solution of the equation $G(\phi_c) = 0$ with $\phi_c \in (0, 2\pi]$, where the function $G(\phi_c)$ is written as

$$G(\phi_c) = \epsilon \cos(\phi_n + \phi_c) - \epsilon \cos(\phi_n) - V_n^* \phi_c. \quad (3)$$

Let us now discuss the origin of the function $G(\phi_c)$ and its physical implications. Between two collisions of the particle with the moving wall, the particle travels with a constant velocity, thanks to the absence of any potential gradient along the way the particle goes. Thus, the position of the particle is given by a linear equation in time. Besides, the vibrating motion of the moving wall turns out impossible to find an analytical expression of the instant of the impact. Therefore, the function $G(\phi_c)$ is obtained as an attempt to account the condition that the position of the particle is the same as the position of the moving wall at the instant of the impact.

If the function $G(\phi_c)$ does not have a root in the interval $\phi_c \in (0, 2\pi]$, we concluded that the particle left the collision zone and a multiple collision no longer happened.

Let us move on and consider now the case of single collisions. In this case, after a collision, the particle leaves the collision zone without a further collision. It returns back due to the fixed wall, which rebound it back to the moving wall. The corresponding expressions used in mapping (2) are $V_n^* = V_n$ and $\Delta T_n = \phi_r + \phi_l + \phi_c$, where the auxiliary terms are given by $\phi_r = (1 - \epsilon \cos(\phi_n))/V_n$ and $\phi_l = (1 - \epsilon)/V_n$. The expression of ϕ_r denotes the time that the particle spends travelling to the right-hand side until it hits the fixed wall. The particle thus suffers an elastic collision and is reflected backwards with velocity $-V_n$. The term ϕ_l denotes the time that the particle spends to enter the collision zone. Finally, ϕ_c is numerically obtained as the smallest solution of the equation $F(\phi_c) = 0$ with $F(\phi_c)$ given by

$$F(\phi_c) = \epsilon \cos(\phi_n + \phi_r + \phi_l + \phi_c) - \epsilon + V_n^* \phi_c. \quad (4)$$

The same discussion used for the function $G(\phi_c)$ also holds here for the function $F(\phi_c)$. Thus, Eq. (4) comes from the condition that the position of the particle is the same as that of the moving wall at the instant of the impact.

Figure 1 shows the phase space for three different values of ϵ and considering 50 different initial conditions. One sees the phase space presents a mixed structure for all values of ϵ . In evidence, there is an existence of the chaotic sea in the low energy regime (below the invariant spanning curve), and then a chain of islands appear as the velocity is increased. After that, the presence of a first invariant spanning curve (FISC), prevents further growth of energy for orbits in the chaotic sea. The position of the FISC varies with ϵ , and an analytical estimation for its position, by using a connection with well known standard mapping² can be found in Ref. 46. Considering the results obtained in the above mentioned papers, the position of FISC is estimated as

$$V_{FISC} = 2\sqrt{\frac{\epsilon}{K_c}} \approx 2\sqrt{\epsilon}, \quad (5)$$

where ϵ is the control parameter and $K_c \approx 0.9716\dots$ is the critical value for the parameter in the standard map,⁴⁷ where the system suffers a transition from local chaos to globally chaotic dynamics.

Analyzing the mixed phase space of the model, we can see that, depending of the initial condition, distinct kinds of dynamics may be observed. If a particle has an initial velocity above V_{FISC} , it cannot cross the curve downwards and stays forever confined to a region of local chaos. The dynamics can then be periodic or chaotic. On the other hand, if the particle has initial velocity below V_{FISC} , the particle has access to more regions in the phase space. This last scenario shows itself more interesting to study, since the dynamical trapping producing the stickiness phenomenon is observed and affects the dynamics and hence the diffusion. Still, we can set that in this dynamical regime, there is a limited region for the particle to have access. The upper barrier is near V_{FISC} and lower limit is chosen to be 0, although there are few observations of velocities reaching $V_n < 0$, mostly dominated by successive collisions. Therefore, in practical terms, we consider the two limits $V_u = V_{FISC}$ and $V_d = 0$.

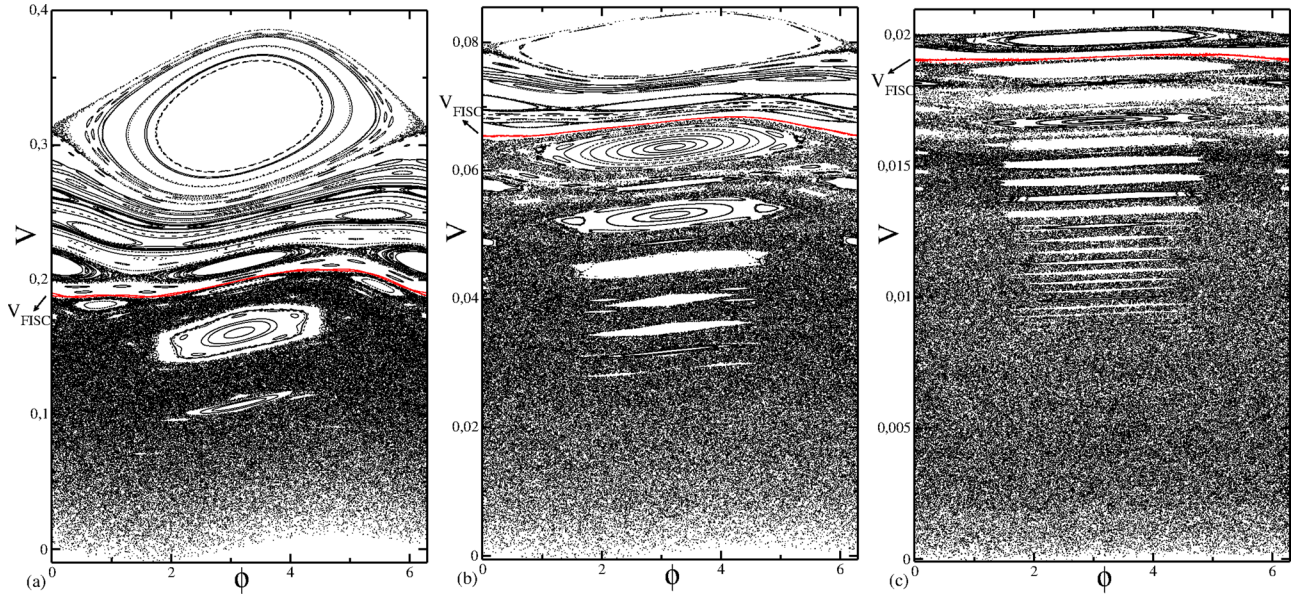


FIG. 1. Phase space for the Fermi-Ulam model described by mapping (2). The control parameters used were: (a) $\epsilon = 10^{-2}$; (b) $\epsilon = 10^{-3}$; and (c) $\epsilon = 10^{-4}$. The gray (red) curve marks the position of the first invariant spanning curve (FISC) in the phase space.

In this limited phase space, the period-one fixed points, $(V^* \phi^*)$, are given by

$$\phi^* = \left\{ \begin{matrix} 0 \\ \pi \end{matrix} \right\}, \quad V^* = \frac{1 - \epsilon \cos(\phi^*)}{m\pi}. \quad (6)$$

The elliptical fixed points (stability islands) are characterized by $\phi^* = \pi$, and $V^* = (1 + \epsilon)/m\pi$, where m is an integer $m = 1, 2, 3, \dots$. They are elliptic as soon as the condition

$$m \geq \frac{1}{\pi} \sqrt{\frac{1 + \epsilon}{\epsilon}} \quad (7)$$

is matched.

III. RESULTS AND DISCUSSION

In this section, we proceed with a statistical analysis for the dynamics of the model. Because of the sine function present in the mapping (2), a direct average over an ensemble of different ϕ is not convenient. Instead, we look at the squared velocity, hence allowing us to estimate the behavior of average squared velocity as function of n . We also discuss the decay rates for the survival probability, and, using a solution of the diffusion equation, we find out an expression for the diffusion coefficient. Our numerical results confirm well the robustness of the theory giving a good agreement of the two.

A. Root mean square velocity (V_{RMS})

To start with, let us investigate the behavior of the averaged square velocity over the dynamical evolution in the number of collisions. From the first equation of mapping (2), and after applying square from both sides, we have $\overline{(V_{n+1})^2} = \overline{(V_n)^2} - 4V_n\epsilon \sin(\phi_{n+1}) + 4\epsilon^2 \sin^2(\phi_{n+1})$. Defining $(\Delta V)^2 = \overline{(V_{n+1})^2} - \overline{(V_n)^2}$, and considering the average in the

interval $\phi \in [0, 2\pi]$ for the terms depending of the phase, which is zero for $\sin(\phi_{n+1})$, and $1/2$ for $\sin^2(\phi_{n+1})$, we end up with

$$(\Delta V)^2 = 2\epsilon^2. \quad (8)$$

Note that we here neglect correlations between ϕ_{n+1} and V_n , since V changes very little from one collision to the next.

In our dynamical analysis, we check the velocity properties between collisions. So, taking the expression of $(\Delta V)^2$ in the interval between collisions, we may interpret this interval as an integration variable,^{48,49} where one may set that

$$\frac{\overline{(V_{n+1})^2} - \overline{(V_n)^2}}{(n+1) - n} \approx \frac{\partial \overline{V^2}}{\partial n}. \quad (9)$$

Integrating both sides, we obtain

$$\int_{V_0}^{V_n} d\overline{V^2} = \int_0^n 2\epsilon^2 dn \rightarrow \overline{(V_n)^2} = (V_0)^2 + 2\epsilon^2 n. \quad (10)$$

For a better statistics, we set $V_{RMS} = \sqrt{\overline{V^2}}$. Then, an analytical expression for the velocity as a function of n is

$$V_{RMS} = \sqrt{(V_0)^2 + 2\epsilon^2 n}, \quad (11)$$

where V_0 is the initial velocity. Of course this expression is not valid for any n , particularly the larger ones. Equation (11) is valid only for small n . Once the phase space is limited by invariant curves, an orbit in the low velocity regime cannot reach regions above the invariant curve for long time dynamics. If we literally take Eq. (11), as n is increased, V_{RMS} should also grows infinitely, and that is not what happens.

We can estimate the window of validity of Eq. (11) by using Eq. (5). Indeed, when $V_{FISC} = V_{RMS}$, we can estimate the number of collisions, n_x critical to where the Eq. (11) is valid. If we choose $V_0 \rightarrow 0$, we obtain $n_x \cong 2/\epsilon$. The relevant

scaling for this crossover is given by $n_x \propto \epsilon^{-1}$, obtained here by simplest way and which is in well agreement with the result known from the literature.²⁷

Let us move ahead and discuss the numerical behavior for V_{RMS} and hence, compare with Eq. (11). First, we evaluated numerically the following expression:

$$\overline{V^2} = \frac{1}{M} \sum_{i=1}^M \frac{1}{n} \sum_{j=1}^n V_{ij}^2, \quad (12)$$

where M is the ensemble of initial conditions, and n is the number of collisions. In a statistical point of view, we take the average of the velocity V_{ij} along the orbit running j and also along the ensemble of initial conditions running i . Initial conditions were always chosen in the chaotic sea with a low initial velocity $V_0 \approx \epsilon$. This was made to warrant a maximum diffusion for a chaotic particle.

Figure 2 shows the behavior for the curves of V_{RMS} as function of n evaluated over an ensemble of 2.000 initial conditions. Each one of them was evolved up to 10^7 collisions with the moving wall. For large enough n , all curves approach to the stationary state marked by V_{SS} . Our result obtained in Eq. (11) shows that when n is small and, considering a negligible initial velocity, i.e., $V_0 \cong 0$, all curves must diffuse with a \sqrt{n} . Hence, $V_{RMS} \propto n^\beta$, where $\beta \approx 1/2$. For large enough n , the curves must converge to the stationary state, which scales as $V_{SS} \propto \epsilon^{1/2}$, as dictated by the position of the lowest invariant spanning curve. The crossing of V_{SS} with V_{RMS} gives a crossover $n_x \propto \epsilon^{-1}$, as we mentioned above.

B. Transport and diffusion

To discuss the diffusion, let us introduce properly a hole in the system. Indeed, we set up a velocity $V_{hole} < V_{FISC}$ that is used to terminate the dynamics. Starting an initial condition with $V_0 \cong 0$, the dynamics evolves and the orbit starts its diffusion along the phase space. When it reaches and hence crosses V_{hole} , the dynamics is terminated, the number

of collisions until that point is annotated, and a new initial condition, with the same velocity and different initial phase, is started. The procedure repeats until all the ensemble is exhausted. The diffusion equation (see Eq. (1)) written specifically to investigate the dynamics of Eq. (2) takes the form

$$\frac{\partial \rho(V, n)}{\partial n} = D \nabla^2 \rho(V, n), \quad (13)$$

where the generic action variable is now set as the particle's velocity V , and the time is measured as the number of collisions n . The diffusion equation setup in (13) only holds for $n \gg 1$, since diffusive process occurs in the chaotic sea for long times. To solve Eq. (13), we use the method of separation variables for a partial differential equation, yielding $\rho(V, n) = U(V)T(n)$. So, applying this to Eq. (13), we obtain as solution for the n variable

$$T(n) = C_1 e^{-\zeta n}, \quad (14)$$

where C_1 is a constant. Also, considering the equation related with the velocity, one may find

$$\frac{U''(V)}{U(V)} = -\frac{\zeta}{D} = -\eta^2. \quad (15)$$

Equation (15) is an ordinary second order differential equation with constant coefficients. Solutions are given in terms of sines and cosines. The boundary conditions are $\frac{\partial \rho(V, n)}{\partial V} = 0$, where, when $V = 0$, we have $U'(0) = 0$; and $\rho(V, n) = 0$, when $V = V_{hole}$. This condition sets that $U(V_{hole}) = 0$, where V_{hole} is the pre-defined escape velocity.

Physically, we can interpret the boundary conditions as being the conservation of particles of the initial ensemble since no particle escaped yet, and the division of the phase space, in orbits that escaped and orbits that did not escaped yet.

Incorporating these into Eq. (15) and considering only odd solutions, we end up with the condition $\eta V_l = l\pi/2$, where $l = 1, 3, 5, \dots$ is sum index of the Fourier series expansion. Since $\eta_l^2 = \zeta_l/D$, we obtain $D = (4V_{hole}^2 \zeta_l)/(l^2 \pi^2)$. Considering yet $V_{hole} = h$ and a change in the notation of the sum index from the Fourier series expansion, from $l/2$ to $(k + 1/2)$, where odd and even terms are considered, one can obtain⁴²

$$\rho(V, n) = \sum_{k=0}^{\infty} A_k \cos \left[\frac{V_k \pi}{h} \left(k + \frac{1}{2} \right) \right] \times \exp \left[\frac{-\pi^2 D n}{h^2} \left(k + \frac{1}{2} \right)^2 \right], \quad (16)$$

where the diffusion coefficient is defined as

$$D = \frac{4h^2 \zeta_k}{\pi^2 (k + 1/2)^2}. \quad (17)$$

The expression given by Eq. (16) furnishes an analytical approximation for the survival probability, when a hole is

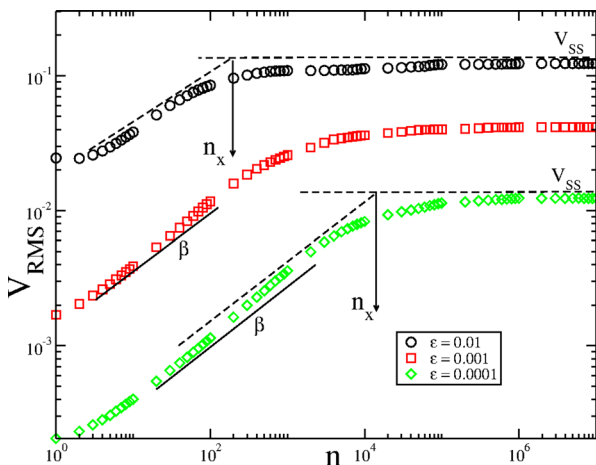


FIG. 2. Plot of the curves for V_{RMS} as a function of n for different values of ϵ . We notice the curves start to grow for short n according to the correct scaling exponent $\beta = 1/2$ and then suffer a changeover after a crossover n_x and bend towards a stationary state V_{SS} for long times.

introduced in the chaotic sea.⁴² This expression holds for any value of k , it just depends on how many terms one would consider in the Fourier series expansion. And for $k = 0$, one could obtain the slowest decay. Also, it is important to clarify that the expression given in Eq. (16) describes well the behavior for the curves of P_{surv} only for an exponential decay. For the case, where it goes through a mixed phase space, the solution of the diffusion equations is more complicated, and is still considered an open problem.

C. Numerical treatment

Let us now discuss our numerical results. When we consider transport properties and diffusion for chaotic dynamics,^{28–33} one can obtain the following expression:

$$\langle [r(n) - r(0)]^2 \rangle = \int r(n)^2 \rho(\vec{r}, n) d\vec{r} = 2Dn, \quad (18)$$

where r is the generic action variable of the system, D is the diffusion coefficient, n is the iteration number, and $\rho(\vec{r}, n)$ is the probability distribution of a system.

For the FUM case, we can use in the expression given by Eq. (18), the previously obtained result in Subsection III A, which is $\langle (\Delta V)^2 \rangle = 2\epsilon^2$. This procedure is made in order to obtain a numerical approximation for the diffusion coefficient. Thus, at each collision of the particle with the moving wall, we calculate the value of the root mean square velocity, or second moment of the dispersion, as

$$\langle \Delta V^2 \rangle = \lim_{NP \rightarrow \infty} \frac{1}{NP} \sum_{i=1}^{NP} (V_n^i - V_0^i)^2, \quad (19)$$

where NP is the number of particles, the index i denotes the NP particles, and V_n is the velocity after n iteration of the i th particle. So, the diffusion coefficient, should be given as

$$D = \lim_{n \rightarrow \infty} \frac{1}{2n} \langle \Delta V^2 \rangle. \quad (20)$$

Figure 3(a) shows a plot of the diffusion coefficient obtained from Eq. (20) as a function of n for $NP = 10^6$. When we compare the relation between the diffusion coefficient and $\langle (\Delta V)^2 \rangle$, i.e., $D = \epsilon^2$ as displayed in Fig. 3(b) in a log-log plot, we found that a power law fitting furnishes $D = 0.974(\epsilon^2)^\delta$, where $\delta \approx 1$. This result remarkably corroborates the linear dependence between D and ϵ^2 , as predicted by Eqs. (8) and (20).

In order to give a more robust result, let us compare with the diffusion expression given in Eq. (17). We considered ten distinct holes equally distributed along the velocity axis, from 2ϵ and the value of V_{SS} , i.e., the value of stationary state for V_{RMS} . Here, we considered the evolution of 10^6 different initial conditions distributed along the phase $\in [0, 2\pi]$ and with $V_0 = 1.1\epsilon$. The behavior of ρ as a function of n is shown in Fig. 4(a).

One can see that as we increase the position of the hole in the velocity axis, which means that we are increasing the possibility of the particle to visit a larger region along the chaotic sea and that the particle has availability to diffuse

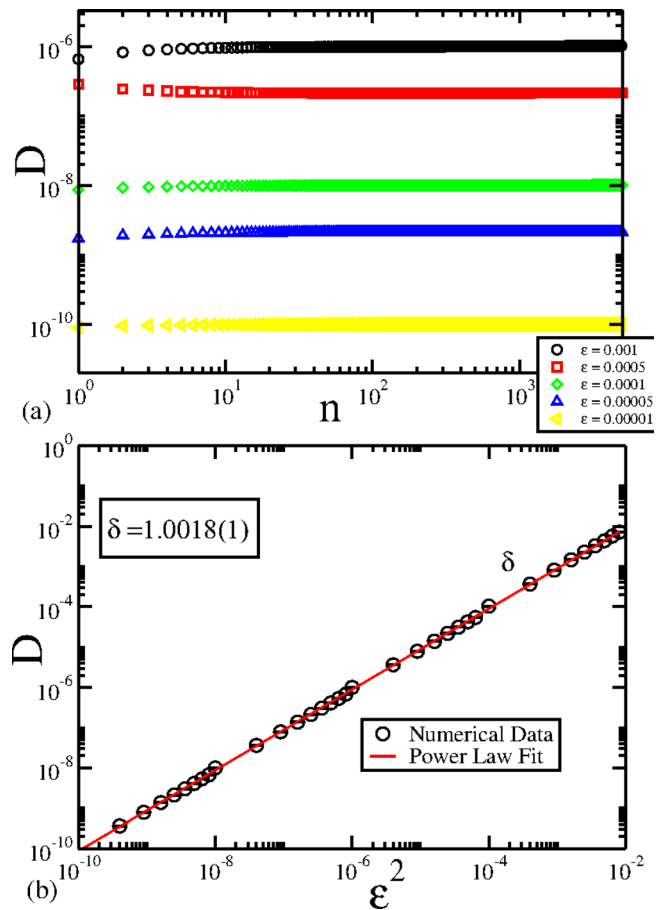


FIG. 3. (a) Plot of the diffusion coefficient D , Eq. (20) as a function of n for different values of ϵ , as labeled in the figure. (b) Plot of D vs ϵ^2 , where a power law fitting furnishes a slope $\delta \approx 1$, thus confirming the relation obtained in Eqs. (8) and (20).

before escape, the exponential decay ζ is slower. This is a clear confirmation that the orbits experience the dynamical trapping yielding in a stickiness, hence producing a slower decay. Indeed, any slower decay than a regular exponential could be addressed to stickiness influence in the dynamics. One could fit a stretched exponential or a power law fit, according to the decay rate of the survival probability. It is still an open problem if a system will present decay rate as a power law or as a stretched exponential as stickiness influence. For the FUM system, we observed a power law decay.

In Figure 4(b), we show a plot of the diffusion coefficient as a function of the position of the hole for 10 different holes located along the phase space and considering different values of ϵ . This was made using the analytical expression given by Eq. (17), for $k = 1$. Here, we used the exponent ζ obtained from every exponential fit in the curves of ρ shown in Fig. 4(a). One could notice that there is a remarkably good agreement between the values of the diffusion coefficient, for the same values of ϵ , between Figs. 3(a) and 4(b), which gives support to the connection of the theory and the numerical data.

Finally, in Fig. 4(c), we rescale the vertical axis by the transformation $D \rightarrow D/\epsilon^2$ and the horizontal axis by $h \rightarrow h/\epsilon$. After this, we obtain an overlap all curves of the diffusion independent of the analyzed hole. We can see

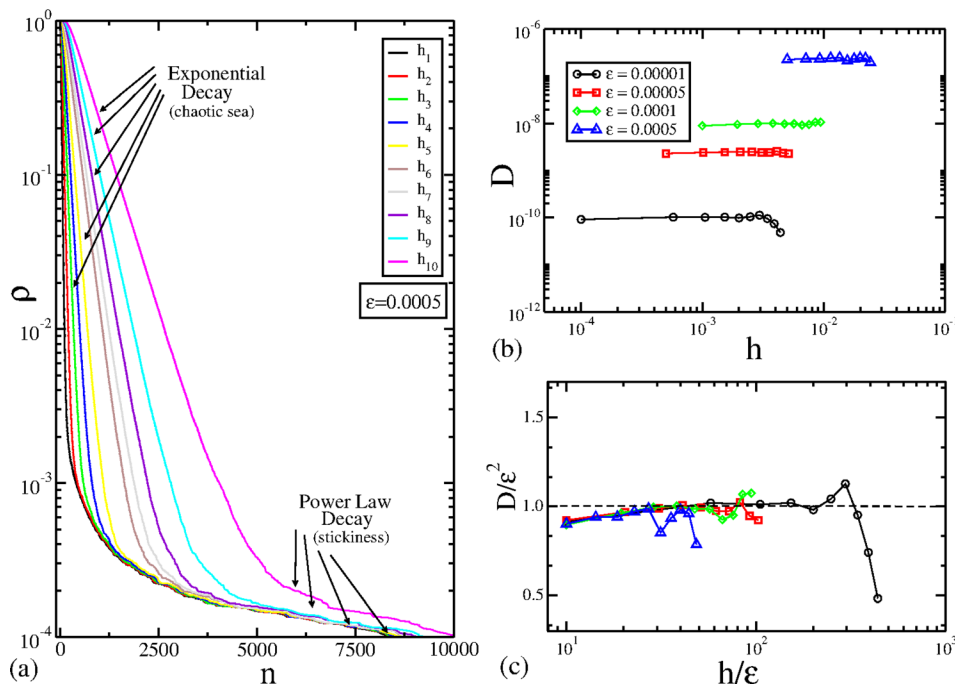


FIG. 4. (a) Plot of the curves of ρ as function of n for 10 distinct positions for the holes considering $\epsilon = 0.0005$. (b) The behavior of the diffusion coefficient given by Eq. (17), as function of the position of the holes h . In (c), a rescale considering $D \rightarrow D/\epsilon^2$ to the curves shown in (b) overlaps all curves around 1 for small values of the scaled variable h/ϵ .

that the rescale in the average for D/ϵ^2 relation is near by 1 (dashed line), which is also in agreement with Eqs. (8) and (20).

The fluctuations around 1 observed in Fig. 4(c) are due to the direct influence of the periodic islands in the phase space, producing then a stickiness near periodic regions in the dynamics. Once the holes were set between 2ϵ and the V_{SS} , for higher holes, there are some stability islands near V_{SS} , so the dynamical trapping becomes inherent in the system. Also, these orbits cause anomalous diffusion influencing also the transport^{3,4} along the chaotic sea. A more complete analytical analysis of the influence of stickiness in the dynamics, particularly near the periodic islands, is still lacking.

IV. FINAL REMARKS AND CONCLUSIONS

In this paper, we studied the dynamics of a particle, or an ensemble of non-interacting particles, confined between two walls, where one is fixed and the other one is periodically perturbed. The dynamics was described by a two-dimensional, nonlinear, transcendental, and measure preserving mapping. The phase space is composed by chaotic seas, KAM islands, and invariant tori, which separates different regions in the phase space. Analyzing the expression for the root mean square velocity as function of n , we estimated analytically the behavior of V_{RMS} .

Considering the transport properties and an analytical analysis of the survival probability ρ , we found an expression for the diffusion coefficient D . From a Fourier series expansion, we have shown that D depends on the exponential rate decay of ρ and also from the hole position in the phase space. A numerical simulation was made and shown to agree well with this expression, confirming the relation between the diffusion coefficient and ϵ^2 , as predicted by Eqs. (8) and (20). Also, we rescaled the behavior of the diffusion

coefficient for 10 different holes, and found a normalization around 1 for D/ϵ^2 , which also agrees with the theory.

Both analytical and numerical results in this paper give robustness to the theory of diffusion analysis, concerning the survival probability curves, as shown also in Ref. 42. In the future, it would be interesting to try to expand this formalism to other more complex dynamical systems, like billiards for instance. Also, to investigate some possible higher order effects in the Fourier series expansion for the analytical expression of diffusion coefficient in Eq. (16), as, for example, $k > 1$, and its effects to Eq. (17), would be an extension of the formalism here presented. Besides, we could try to estimate numerically Eq. (16) behavior and possible stickiness influence to this analysis.

ACKNOWLEDGMENTS

A.L.P.L. acknowledges FAPESP (2014/25316-3) and CNPq for financial support. I.L.C. thanks FAPESP (2011/19296-1) and E.D.L. thanks FAPESP (2012/23688-5), CNPq and CAPES, Brazilian agencies. A.L.P.L. also thanks the University of Bristol for the kind hospitality during his stay in UK. All authors thank the anonymous referees for many helpful comments. This research was supported by resources supplied by the Center for Scientific Computing (NCC/GridUNESP) of the São Paulo State University (UNESP).

¹R. C. Hilborn, *Chaos and Nonlinear Dynamics: An Introduction for Scientists and Engineers* (Oxford University Press, New York, 1994).

²A. J. Lichtenberg and M. A. Leiberman, *Regular and Chaotic Dynamics*, Applied Mathematical Sciences Vol. 38 (Springer Verlag, New York, 1992).

³G. M. Zaslavsky, *Physics of Chaos in Hamiltonian Systems* (Imperial College Press, New York, 2007).

⁴G. M. Zaslavsky, *Hamiltonian Chaos and Fractional Dynamics* (Oxford University Press, New York, 2008).

⁵G. Contopoulos, *Astrophys. J.* **76**, 147 (1971).

⁶D. del-Castillo-Negrete, B. A. Carreras, and V. E. Lynch, *Phys. Rev. Lett.* **94**, 065003 (2005).

- ⁷J. S. E. Portela, I. L. Caldas, and R. L. Viana, *Int. J. Bifurcation Chaos* **17**, 4067 (2007).
- ⁸E. G. Altmann, *Phys. Rev. A* **79**, 013830 (2009).
- ⁹G. Contopoulos and M. Harsoula, *Celestial Mech. Dyn. Astron.* **107**, 77 (2010).
- ¹⁰T. Tél, A. de Moura, C. Grebogi, and G. Krolyi, *Phys. Rep.* **413**, 91 (2005).
- ¹¹E. G. Altmann, J. S. E. Portela, and T. Tél, *Rev. Mod. Phys.* **85**, 869 (2013).
- ¹²S. M. Ulam, *A Collection of Mathematical Problems*, Interscience Tracts in Pure and Applied Mathematics Vol. 8 (Interscience Publishers, New York-London, 1960).
- ¹³E. Fermi, *Phys. Rev.* **75**, 1169 (1949).
- ¹⁴A. K. Karlis, P. K. Papachristou, F. K. Diakonou, V. Constantoudis, and P. Schmelcher, *Phys. Rev. Lett.* **97**, 194102 (2006).
- ¹⁵A. K. Karlis, P. K. Papachristou, F. K. Diakonou, V. Constantoudis, and P. Schmelcher, *Phys. Rev. E* **76**, 016214 (2007).
- ¹⁶D. F. M. Oliveira and E. D. Leonel, *New J. Phys.* **13**, 123012 (2011).
- ¹⁷D. F. M. Oliveira and E. D. Leonel, *Physica A* **392**, 1762 (2013).
- ¹⁸D. F. Tavares, E. D. Leonel, and R. N. Costa Filho, *Physica A* **391**, 5366 (2012).
- ¹⁹A. Veltri and V. Carbone, *Phys. Rev. Lett.* **92**, 143901 (2004).
- ²⁰F. Saif, I. Bialynicki-Birula, M. Fortunato, and W. P. Schleich, *Phys. Rev. A* **58**, 4779 (1998).
- ²¹A. Steane, P. Szriftgiser, P. Desbiolles, and J. Dalibard, *Phys. Rev. Lett.* **74**, 4972 (1995).
- ²²S. T. Dembinski, A. J. Makowski, and P. Peplowski, *Phys. Rev. Lett.* **70**, 1093 (1993).
- ²³J. V. Jos and R. Cordery, *Phys. Rev. Lett.* **56**, 290 (1986).
- ²⁴F. Saif and I. Rehman, *Phys. Rev. A* **75**, 043610 (2007).
- ²⁵Z. J. Kowalik, M. Franaszek, and P. Pieranski, *Phys. Rev. A* **37**, 4016 (1988).
- ²⁶S. Warr, W. Cooke, R. C. Ball, and J. M. Huntley, *Physica A* **231**, 551 (1996).
- ²⁷E. D. Leonel, P. V. E. McClintock, and J. K. L. da Silva, *Phys. Rev. Lett.* **93**, 014101 (2004).
- ²⁸P. Gaspard, *Chaos, Scattering and Statistical Mechanics* (Cambridge University Press, Cambridge, 1998).
- ²⁹R. K. Pathria, *Statistical Mechanics* (Elsevier, Burlington, 2008).
- ³⁰P. Gaspard, *Chaos* **3**, 427 (1993).
- ³¹J. R. Dorfman and P. Gaspard, *Phys. Rev. E* **51**, 28 (1995).
- ³²T. Tél, J. Vollmer, and W. Breymann, *Europhys Lett.* **35**, 659 (1996).
- ³³F. Borgonovi, I. Guarneri, and D. L. Shepelyansky, *Phys. Rev. A* **43**, 4517 (1991).
- ³⁴P. Gaspard and G. Nicolis, *Phys. Rev. Lett.* **65**, 1693 (1990).
- ³⁵P. Gaspard and D. Alonso Ramirez, *Phys. Rev. A* **45**, 8383 (1992).
- ³⁶A. L. P. Livorati, T. Kroetz, C. P. Dettmann, I. L. Caldas, and E. D. Leonel, *Phys. Rev. E* **86**, 036203 (2012).
- ³⁷E. D. Leonel and C. P. Dettmann, *Phys. Lett. A* **376**, 1669 (2012).
- ³⁸C. P. Dettmann and E. D. Leonel, *Physica D* **241**, 403 (2012).
- ³⁹G. Knight, O. Georgiou, C. P. Dettmann, and R. Klages, *Chaos* **22**, 023132 (2012).
- ⁴⁰O. Georgiou, C. P. Dettmann, and E. G. Altmann, *Chaos* **22**, 043115 (2012).
- ⁴¹A. L. P. Livorati, O. Georgiou, C. P. Dettmann, and E. D. Leonel, *Phys. Rev. E* **89**, 052913 (2014).
- ⁴²J. A. de Oliveira, C. P. Dettmann, D. R. Costa, and E. D. Leonel, *Phys. Rev. E* **87**, 062904 (2013).
- ⁴³D. G. Ladeira and E. D. Leonel, *Phys. Rev. E* **81**, 036216 (2010).
- ⁴⁴D. F. M. Oliveira and M. Robnik, *Phys. Rev. E* **83**, 026202 (2011).
- ⁴⁵M. R. Silva, D. R. da Costa, and E. D. Leonel, *J. Phys. A* **45**, 265101 (2012).
- ⁴⁶E. D. Leonel, J. A. de Oliveira, and F. Saif, *J. Phys. A* **44**, 302001 (2011).
- ⁴⁷B. V. Chirikov, *Phys. Rep.* **52**, 263 (1979).
- ⁴⁸E. D. Leonel, A. L. P. Livorati, and A. M. Cespedes, *Physica A* **404**, 279 (2014).
- ⁴⁹E. D. Leonel and A. L. P. Livorati, *Commun. Nonlinear Sci. Numer. Simul.* **20**, 159 (2015).